ACS APPLIED MATERIALS & INTERFACES

Research Article

www.acsami.org

Alkyl Chain Length Dependence of the Field-Effect Mobility in Novel Anthracene Derivatives

Jang Yeol Back,[†,⊥] Tae Kyu An,[‡,⊥] Ye Rim Cheon,[§] Hyojung Cha,[‡] Jaeyoung Jang,[‡] Yebyeol Kim,[‡] Yonghwa Baek,[‡] Dae Sung Chung,[∥] Soon-Ki Kwon,*[,†] Chan Eon Park,*[,‡] and Yun-Hi Kim*[,§]

[†]School of Materials Science & Engineering, Engineering Research Institute (ERI), Gyeongsang National University, Jinju 660-701, Republic of Korea

[‡]Polymer Research Institute, Department of Chemical Engineering, Pohang University of Science and Technology (POSTECH), Pohang 790-784, Republic of Korea

[§]Department of Chemistry & Engineering Research Institute (ERI), Gyeongsang National University, Jinju 660-701, Republic of Korea

[∥]School of Chemical Engineering and Material Science, Chung-Ang University, Seoul 156-756, Republic of Korea

Supporting Information

ABSTRACT: We report six asymmetric alkylated anthracene-based molecules with different alkyl side chain lengths for use in organic field-effect transistors (OFETs). Alkyl side chains can potentially improve the solubility and processability of anthracene derivatives. The crystallinity and charge mobility of the anthracene derivatives may be improved by optimizing the side chain length. The highest field-effect mobility of the devices prepared here was 0.55 $cm^2/(V\ s)$, for 2-(*p*-pentylphenylethynyl)anthracene (PPEA). The moderate side chain length appeared to be optimal for promoting self-organization among asymmetric anthracene derivatives in OFETs, and was certainly better than the short or long alkyl side chain lengths, as confirmed by X-ray diffraction measurements.

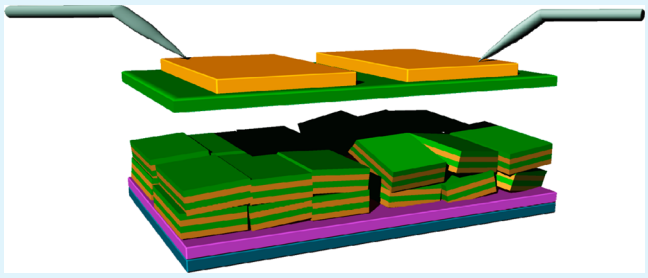

KEYWORDS: *organic field-effect transistor (OFET), alkyl chain length, asymmetric anthracene, structure−mobility relationship, crystal orientation*

INTRODUCTION

Over the past two decades, organic electronics, such as organic field-effect transistors (OFETs),[1,2] organic light emitting diodes (OLEDs),[3,4] organic photovoltaic cells (OPVs),[5,6] and organic photodetectors (OPDs),[7,8] have received significant attention for use in flexible low-cost electronics applications.[9−12] In these fields of research, OFETs have been developed to act as amplifying and switching devices.[13,14] The commercialization of high-performance OFETs will require several issues to be addressed, including increasing the field-effect mobility,[15] improving operation stability,[16,17] developing passivation methods,[18,19] and improving performance reproducibility.[20,21] A variety of efforts have been applied toward solving these problems. The molecular design of organic semiconductors offers a useful strategy for solving these problems because tailoring the molecular structures can change the properties of the organic semiconductors dramatically.[22,23] Many classes of conjugated molecules and polymers have been synthesized, their electrochemical properties have been investigated[24,25] and they have been found to display high performances and offer chemically stable conjugated systems.[26−28]

The class of acene-based molecules shows promise for use as the active material in organic semiconductors and in OFETs, in particular, because the extended π-systems of the acene units can engage in strong intermolecular overlap in the thin film state, yielding a high field-effect mobility.[29−32] Many research groups have examined the structure-performance relationships in acene-based molecules.[33−36] Most efforts have focused on tuning the conjugated core backbones of the acene-based molecules because the main core unit determines the electrical and chemical properties, including the polarizability, stability toward oxidation, energy level and intermolecular interactions.[37−40] We also reported dialkoxynaphthalene end-capped anthracene derivatives and 2-hexylthienothiophene end-capped anthracene derivatives.[41,42] The anthracene derivatives with introduced electron rich end groups showed good stability and mobility due to enhanced $\pi-\pi$ stacking resulting from their densely packed crystal structures.

Recently, more and more attention has been dedicated to controlling alkyl chains in acene-based molecules to improve the intermolecular ordering in the thin film state.[43−45] When functionalized with flexible side groups, these molecules

Received: September 15, 2014
Accepted: December 17, 2014
Published: December 26, 2014

DOI: 10.1021/am5063103
ACS Appl. Mater. Interfaces 2015, 7, 351−358

Scheme 1. Synthesis of the Six Alkylated Anthracene Derivatives

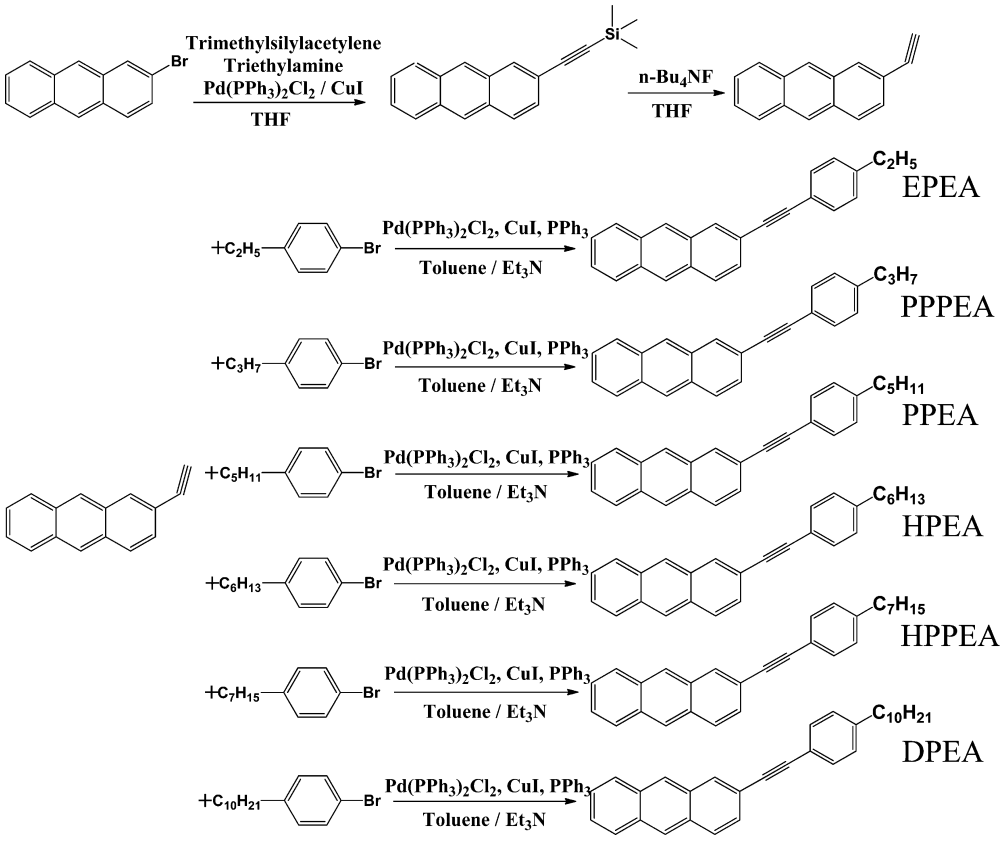

become soluble in common organic solvents and can be applied to solution-process at room temperature.[46] Alkyl side chains have been shown to play an important role in molecular self-organization and thin film packing structures.[47−53] The van der Waals interactions between alkyl side chains can exert a more important influence on the molecular ordering than interactions between conjugated units. Unfortunately, the dependence of the charge carrier mobility on the alkyl chain length in acene-based molecules with asymmetric alkyl chain structures has not been extensively investigated, and many challenges remain toward improving the OFET device performances. We have examined the dependence of the charge carrier mobility on the alkyl chain length in acene-based molecules in an effort to control the packing structures in the thin film.

In this study, we designed and synthesized six novel asymmetric alkylated anthracene-based molecules to uncover the relationship between the alkyl chain length of the asymmetric acene-based molecules and the OFET performance. The alkylphenyl ethynyl group might be extended conjugation of anthracene, leading increased intermolecular interaction without decrease of the chemical stability. The designed molecules tested here are 2-(4-ethyl-phenylethynyl)-anthracene (EPEA), 2-(*p*-propylphenylethynyl)anthracene (PPPEA), 2-(*p*-pentylphenylethynyl)anthracene (PPEA), 2-(4-hexyl-phenylethynyl)anthracene (HPEA), 2-(*p*-heptylphenylethynyl)anthracene (HPPEA), and 2-(p-decylphenylethynyl)anthracene (DPEA), each of which is composed of an anthracene core and an asymmetrically alkylated phenyl ethynyl group. The extended π-conjugated rigid rod structure of the phenyl ethynylated anthracene can facilitate the formation of a high degree of intermolecular ordering,[54,55] leading to high mobility. In addition, the asymmetrically introduced alky side chain can potentially improve the solubility and processability of the anthracene derivatives. We systematically investigated the effects of the alkyl chain length to achieve high electrical performances in OFET devices based on asymmetric acene-based molecules by increasing the linear alkyl units from two to ten. We expect that a higher mobility may be achieved by optimizing the alkyl chain length of the asymmetric acene-based molecules. OFETs based on these molecules were fabricated using a solution process. The field-effect mobility in the PPEA bearing pentyl alkyl chain units was much higher than in the other molecules, which bore chains that were shorter or longer than the pentyl alkyl chain units. The correlation between the alkyl chain length and the mobility is discussed in detail in the context of molecular self-organization.

RESULTS AND DISCUSSION

2.1. Synthesis and Thermal Analysis. The synthetic scheme used to prepare EPEA, PPPEA, PPEA, HPEA, HPPEA, and DPEA is shown in Scheme 1. The anthracene derivatives of the asymmetric structures bearing different alkyl chain lengths were prepared via a desilylation and Sonogashira coupling reaction. The chemical structures of the compounds were confirmed by H NMR and HR-mass spectroscopy analyses.

The thermal stabilities of the obtained compounds were characterized by thermogravimetric analysis (TGA) and differential scanning calorimetry (DSC) (Figures S1 and S2, Supporting Information). All anthracene derivatives exhibited good thermal stability. The 5% decomposition temperature (T_d 5%) of the EPEA, PPPEA, PPEA, HPEA, HPPEA, and DPEA were 284, 301, 298, 321, 334, and 330 °C, respectively. The decomposition temperature was found to increase slightly while

DOI: 10.1021/am5063103
ACS Appl. Mater. Interfaces 2015, 7, 351−358

the melting transition temperature decreased slightly as the alkyl chain length was increased. DSC results indicated that all anthracene derivatives had a sharp melting transition, and the melting temperatures of the EPEA, PPPEA, PPEA, HPEA, HPPEA, and DPEA were 200, 183, 169, 168, 151, and 153 °C, respectively.

2.2. Optical and Electrochemical Properties. We measured the optical absorption spectra of all anthracene derivatives with asymmetric structures in the solution and film states, as shown in Figure 1. All anthracene derivatives in

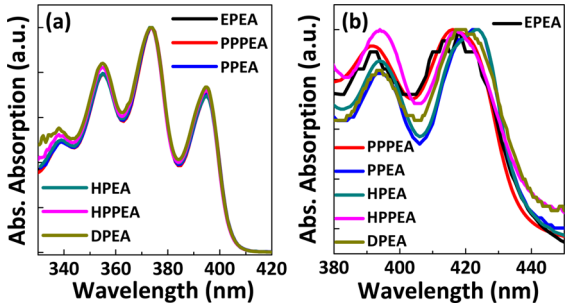

Figure 1. UV−vis absorption spectra of the five anthracene derivatives (a) in chloroform and (b) in the solid state.

solution showed the same absorption maxima at 355, 373, and 395 nm, which are characteristic of the anthracene transition positions because the conjugated segments of the anthracene derivatives were indistinguishable. We discovered that the absorption peaks of the asymmetric molecules in the thin films were almost 25 nm red-shifted relative to those in the solution state (Figure 1). Such spectral shifts arose from changes in the energy levels due to the molecular packing geometry,[56] indicating a greater degree of intermolecular ordering within the anthracene derivatives in the film state.[57]

The electrochemical properties of the films were examined by cyclic voltammetry measurements. The highest occupied molecular orbital (HOMO) energy levels were estimated from the onset points of the oxidation potentials in the cyclic voltammograms and the lowest unoccupied molecular orbital (LUMO) energy levels were calculated from the HOMO energy levels and the E_g values. The calculated energy levels are presented in Table 1. The HOMO energy level of EPEA, PPPEA, PPEA, HPEA, HPPEA, and DPEA were almost similar −5.63∼−5.59 eV. The optical onset of EPEA, PPPEA, PPEA, HPEA, HPPEA, and DPEA was also almost similar 2.81∼2.83 eV.

Table 1. Optical Properties of the Six Anthracene Derivatives

	HOMO (eV)	LUMO (eV)	E_g (eV)[a]
EPEA	5.63	2.81	2.82
PPPEA	5.59	2.77	2.82
PPEA	5.63	2.81	2.82
HPEA	5.59	2.77	2.82
HPPEA	5.62	2.79	2.83
DPEA	5.63	2.80	2.83

[a]E_g: band gap energy calculated from the equation $E_g = hc/\lambda = 1024/\lambda$, where λ is the edge wavelength (nm) of UV−vis absorption spectrum.

2.3. XRD Analysis. Figure 2 shows the XRD patterns obtained from the thin films of the anthracene-based molecules,

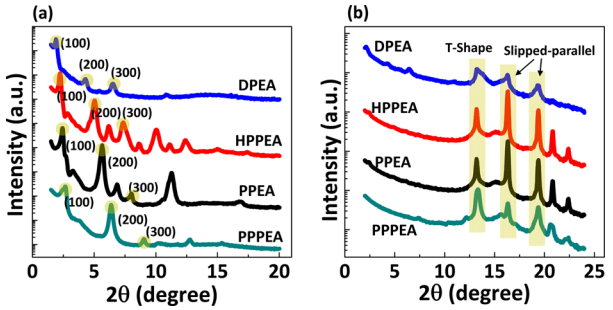

Figure 2. 1D XRD patterns: (a) out-of-plane XRD patterns and (b) in-plane X-ray diffraction patterns.

deposited onto an octyltrichlorosilane (OTS)-treated Si/SiO_2 substrate by spin coating. The first peak positions along the out-of-plane direction in the PPPEA, PPEA, HPPEA, and DPEA films were observed at 2θ = 2.66, 2.44, 2.24, and 1.90°, with interlayer distances of 2.31, 2.52, 2.74, and 3.23 nm, respectively (Figure 3). The XRD data revealed that the interlayer distances depended on the side chain length.

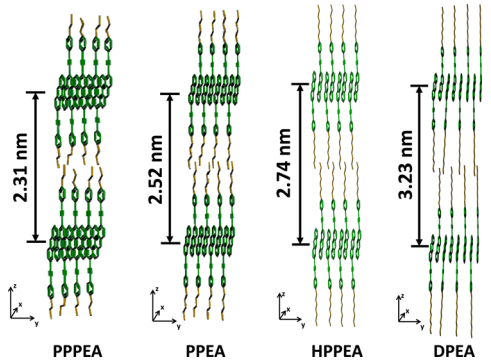

Figure 3. Estimated crystal structure of PPPEA, PPEA, HPPEA, and DPEA.

Along the in-plane direction in the anthracene-based molecular films, three main diffraction peaks were observed, as shown in Figure 4. The peak positions along the in-plane direction in the films were very similar, suggesting that the anthracene−anthracene interactions were independent of the alkyl side chain length. Ordered Bragg peaks along the in-plane direction were observed at 2θ = 13.2°, 16.35°, and 19.4°, corresponding to intermolecular distances of 0.48, 0.38, and 0.32 nm. The intermolecular distance values were difficult to explain in terms of a simple parallel configuration of the molecules. One possibility is that the anthracene-based molecules formed a crystal packing structure through a combination of T-shaped and slipped-parallel configurations, as illustrated in Figure 5. The crystalline structures of the anthracene-based molecules were controlled by the electrostatic interactions between molecules.[58] The energetics of the interactions between anthracene molecules were investigated. The energy states of two energy-minimized configurations were shown to be lower than the energy of a simple parallel configuration.[59]

As shown in Figure 2, the Bragg peak intensities of the PPPEA and DPEA films were weaker than that of other films

DOI: 10.1021/am5063103
ACS Appl. Mater. Interfaces 2015, 7, 351−358

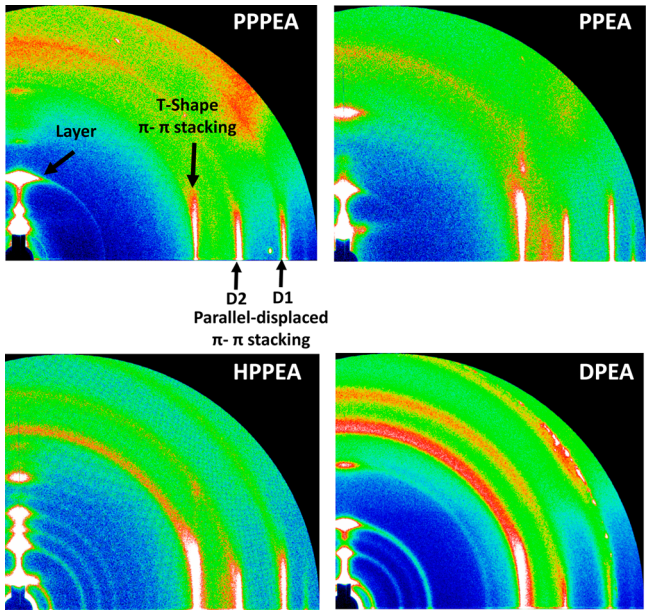

Figure 4. Grazing-incidence wide-angle X-ray scattering (GIWAXS) patterns obtained from thin films prepared from PPPEA, PPEA, HPPEA, and DPEA.

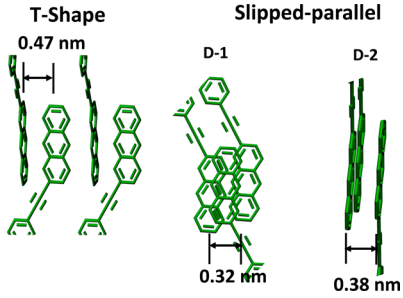

Figure 5. Estimated configurations of the $\pi-\pi$ stacking structure.

composed of PPEA and HPPEA, indicating that the degree of crystallinity in the PPPEA and DPEA films was not as high as that in the PPEA and HPPEA films.[60] The ethyl and propyl side chain units in EPEA and PPPEA limited their solubility in chloroform, and molecular self-organization was precluded in the solid phase. As the side chain length increased, the solubility of the anthracene-based molecules (PPEA and HPEA) improved significantly compared to the solubilities of EPEA and PPPEA. The appropriate side chain length increased the solubility, thereby enabling solution processing and promoting the formation of highly crystalline thin film structures. The well-ordered molecular structures facilitated efficient lateral charge transport along adjacent molecules in the OFET architecture.

As the crystalline film formed, the interactions between aromatic molecules provided the dominant influence on the structure. Excessively long alkyl chains tended to disrupt the balance of intermolecular forces between the cores and between the alkyl chains.[51] Long alkyl chains exacerbated molecular packing in the OFET device architectures. Steric crowding in the side chain distribution induced the formation of an ordered structure through intermolecular alkyl chain interactions. The structural data presented in Figure 4 indicated that an increase in the side chain length, from the pentyl units (PPEA) up to the decyl units (DPEA), was accompanied by increased resolution in the circular scattering patterns, indicating that the fraction of randomly oriented molecules had increased.[61] Molecular packing models of anthracene-based compounds in films are proposed here, as illustrated in Figure 6.

2.4. FET Behavior. The effects of the alkyl chain length in the asymmetric molecule derivatives on the organic semiconductor performance were explored by first fabricating OFETs based on these derivatives using a solution process. As shown in Figure 7, OFET devices composed of asymmetric

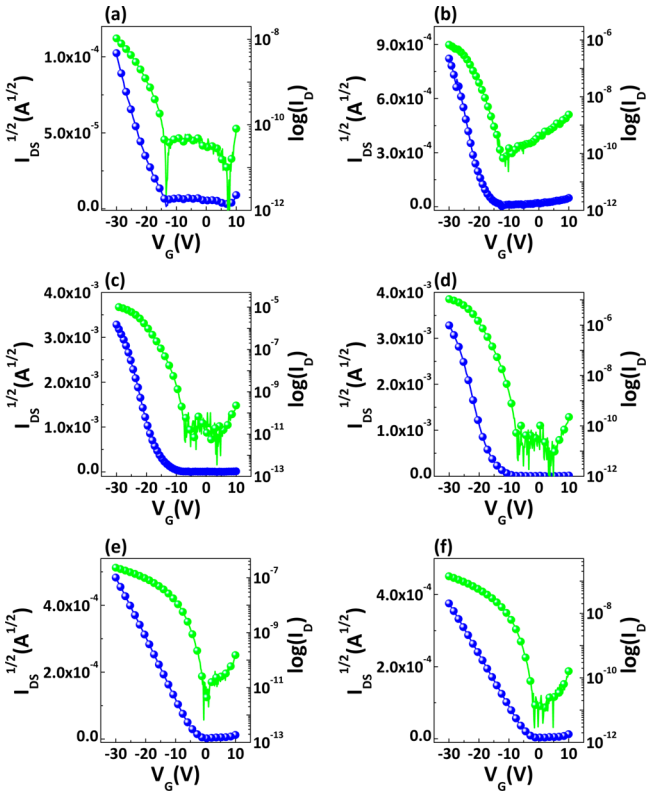

Figure 7. Transfer curves obtained from OFETs prepared from (a) EPEA, (b) PPPEA, (c) PPEA, (d) HPEA, (e) HPPEA, and (f) DPEA.

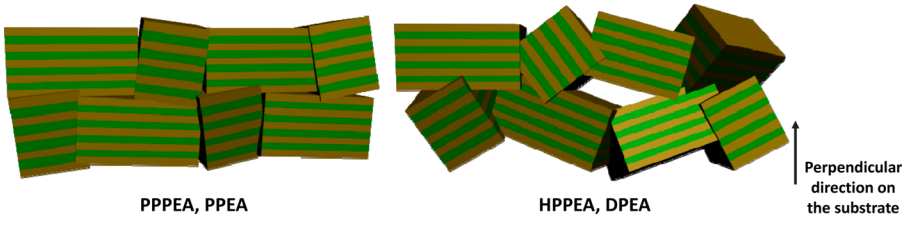

Figure 6. Estimated packing structures for the four anthracene derivatives.

DOI: 10.1021/am5063103
ACS Appl. Mater. Interfaces 2015, 7, 351−358

molecules showed typical *p*-channel responses in the saturation regime. The electrical parameters of the OFETs prepared from asymmetric molecular films are summarized in Table 2.

Table 2. Performance Properties of the Solution-Processed OFET Devices

compounds	mobility ($cm^2/(V\ s)$)	I_{on}/I_{off}	V_{th} (V)	SS (V/dec)
EPEA	3.5×10^{-4}	4.5×10^{3}	−16	0.28
PPPEA	0.046	1.9×10^{4}	−19	0.26
PPEA	0.55	1.9×10^{6}	−16	0.23
HPEA	0.49	1.5×10^{6}	−16	0.25
HPPEA	2.3×10^{-3}	1.8×10^{4}	−3.4	0.31
DPEA	1.4×10^{-3}	1.5×10^{4}	−3.7	0.37

As shown in Figure 8, the field-effect mobilities depended on the asymmetric molecule alkyl chain length. A nonmonotonic

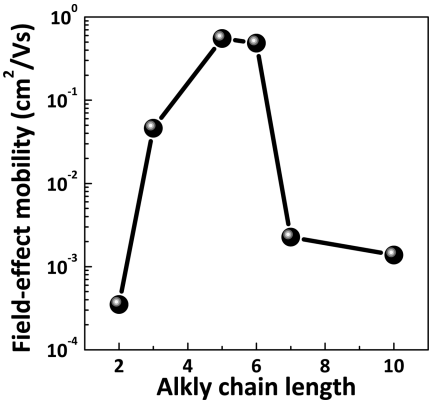

Figure 8. Dependence of the field-effect mobility on the alkyl chain length in asymmetric anthracene derivatives.

trend in the field-effect mobility with the alkyl chain length was observed. A 3 orders of magnitude increase in the field-effect mobility was observed, from 3.5×10^{-4} to 5.5×10^{-1} $cm^2/(V\ s)$, in moving from the ethyl (EPEA) to the pentyl (PPEA) side chains. A sharp decrease in the hole mobility of about 2 orders of magnitude was observed in moving from the heptyl (HPPEA) to the decyl (DPEA) groups (around 10^{-3} $cm^2/(V\ s)$) (Figure 8). The maximum field-effect mobility measured from the PPEA-based OFET was observed among the series of asymmetric molecules.

An excessively short linear alkyl chain did not convey good solubility to the molecule in organic solvents. Poor solubility prevents self-organization and molecular packing in a thin film during the spin-coating process. The semiconducting materials, then, do not readily form uniform and smooth films, and the long-range molecular ordering needed to form carrier percolation pathways is absent. On the other hand, excessively long alkyl chains disrupt the carrier percolation pathways and form randomly oriented crystals, as shown in Figure 6. The long alkyl chains then create bulky insulating layers between the semiconducting $\pi-\pi$ stacks along the polycrystalline thin film that limit the vertical carrier percolation pathways from the source to the drain (injection and extraction). A high fraction of insulating regions in a film matrix can dilute the number of π systems close to the channel interface, thereby reducing the mobility in the OFETs.[62]

CONCLUSIONS

Six anthracene-based molecules were designed and synthesized. The field-effect mobilities were measured as a function of the alkyl chain length by systematically investigating OFETs prepared using thin films of these molecules. We found that the length of the alkyl side chain influenced the ordered molecular packing structure and the field-effect mobility. The mobility varied with the alkyl chain length, reaching its highest value for PPEA. Short alkyl chains could not provide good solubility, which prevented the development of well-ordered structures during solution processing. Long alkyl chains interrupted hole transport and negatively affected the crystalline structures of the molecules. Small changes in the alkyl lengths in the molecular structures dramatically affected the solid-state ordering of these molecules. These results confirmed that the presence of optimized alkyl side chains with asymmetric structures of acene-based molecules enhanced the $\pi-\pi$ stacking and improved the molecular ordering in the solid film state. We conclude that optimization of the alkyl chain length is essential for preparing high-performance OFETs.

EXPERIMENTAL SECTION

Measurements. The ^1H NMR spectra were recorded using an Avance-300 MHz spectrometer. Mass spectra were measured using a Jeol JMC-700 and GCmate2. The thermal analysis measurements were performed using a TA 2050 TGA thermogravimetric analyzer under a nitrogen atmosphere. The samples were heated at 10 °C/min. Differential scanning calorimetry was conducted under nitrogen using a TA Instruments 2100 DSC. The samples were heated at 20 °C/min from 0 to 250 °C. UV−vis absorption spectra were measured using a PerkinElmer LAMBDA-900 UV/vis/IR spectrophotometer. Cyclic voltammograms of materials were recorded on an epsilon E3 at a room temperature in a 0.1 M solution of tetrabutylammonium perchrolate (Bu_4NClO_4) in acetonitrile under nitrogen gas at a scan rate of 50 mV/s. A Pt wire was used as the counter electrode and a $Ag/AgNO_3$ electrode as the reference electrode.

Materials. 2-Bromoanthracene, trimethylsilyl acetylene, copper(I) iodide, tetrabutylammomium fluoride, 1-bromo-4-ethyl-benzene, 1-bromo-4-propyl-benzene, 1-bromo-4-heptyl-benzene, 1-bromo-4-decyl-benzene, and triethylamine were purchased from Aldrich. $Pd(PPh_3)Cl_2$ was purchased from Amicore.

Synthesis. *Anthracen-2-ylethynyl-trimethyl-silane.* 2-Bromo-anthracene (30 g, 0.117 mol), $Pd(PPh_3)_2Cl_2$ (2.5 g, 0.004 mol), and CuI (1.2 g, 0.006 mol) were dissolved in 200 mL of THF. Triethylamine and trimethylsilylacetylene were then slowly added to the mixture, and the mixture was refluxed for 18 h. The reaction was quenched using saturated NH_4Cl, and the organic layer was removed with hexane and dried over $MgSO_4$. After concentration, the residue was purified by column chromatography on silica gel (hexane) to give (anthracen-2-ylethynyl)trimethylsilane as a yellow solid in an 68% yield. ^1H NMR (300 MHz, $CDCl_3$): δ 8.38 (s, 2H), 8.19 (s, 1H), 8.03−7.99 (m, 2H), 7.95−7.92 (d, 1H), 7.52−7.45 (m, 3H), 0.33 (s, 9H). MS (EI) *m/z*: 274 (M^+).

2-Ethynylanthracene. (Anthracen-2-ylethynyl)trimethylsilane (20.00 g, 0.080 mol) was dissolved in THF (600 mL), and tetrabutylammonium fluoride (473.5 mL, 0.43 mol) was added to the solution. The mixture was stirred for 2 h, the reaction was quenched with water, and the organic phase was extracted with ethyl ether. The crude product was purified by column chromatography on a short silica gel column (hexane) and recrystallized in methylene chloride (MC) and hexane (1:1) to yield 2-ethynylanthracene as a yellow solid in 84.81% (12.5 g) yield. mp: 181−182 °C. ^1H NMR (300 MHz, $CDCl_3$): δ 8.41 (s, 2H), 8.22 (s, 1H), 8.03−7.95 (m, 3H), 7.53−7.47 (m, 3H), 3.22 (s, 1H). ^{13}C-NMR (500 MHz, $CDCl_3$, ppm): δ 136.35, 134.18, 133.58, 133.31, 133.25, 130.82, 130.20, 129.48, 129.20, 128.18, 126.44, 126.21, 125.88, 120.52, 85.55, 78.55. MS (EI) *m/z*: 202 (M^+).

DOI: 10.1021/am5063103
ACS Appl. Mater. Interfaces 2015, 7, 351−358

2-(4-Ethyl-phenylethynyl)anthracene (EPEA). 1-Bromo-4-ethyl-benzene (2 g, 0.011 mol), $Pd(PPh_3)_2Cl_2$ (2.9 mg, 0.006 mmol), and CuI (7.6 mg, 0.040 mmol) were dissolved in toluene/triethylamine (20 mL/20 mL). To the mixture was added 2-ethynyl-anthracene (3.28 g, 0.016 mol), and the solution was stirred for 24 h at 90 °C. The crude product was extracted with chloroform and washed with 5 N HCl. It was purified by column chromatography using ethyl acetate/hexane (1:10) as the eluent, and recrystallized using MC and hexane (1:1). Yield: 1.5 g (45.6%). ^{1}H NMR (300 MHz, $CDCl_3$): δ 8.41 (s, 2H), 8.23 (s, 1H), 8.03−7.97 (m, 3H), 7.56−7.48 (m, 5H), 7.25−7.22 (d, 2H), 2.74−2.67 (m, 2H), 1.31−1.23 (t, 3H). HRMS: calcd for $C_{24}H_{18}$: 306.1409. Found: 306.1406.

2-(4-Propyl-phenylethynyl)anthracene (PPPEA). The reaction applied to the synthesis of EPEA was conducted using 1-bromo-4-propyl-benzene. Yield: 2.41 g (75%). ^{1}H NMR (300 MHz, $CDCl_3$): δ 8.41 (s, 2H), 8.23 (s, 1H), 8.03−8.00 (m, 3H), 7.56−7.48 (m, 5H), 7.26−7.20 (d, 2H), 2.66−2.61 (t, 2H), 1.75−1.62 (m, 2H), 1.00−0.95 (t, 3H). HRMS: calcd for $C_{25}H_{20}$: 320.1565. Found: 320.1565.

2-(4-Pentyl-phenylethynyl)anthracene (PPEA). The reaction applied to the synthesis of EPEA was conducted using 1-bromo-4-propyl-benzene. Yield: 0.3 g (39%). ^{1}H NMR (300 MHz, $CDCl_3$): δ 8.41 (s, 2H), 8.24 (s, 1H), 8.05−7.97 (m, 3H), 7.57−7.49 (m, 5H), 7.3 (d, 2H), 2.68 (t, 2H), 1.65−1.58 (m, 2H), 1.34−1.39 (m, 4H), 0.94 (t, 3H). HRMS: calcd for $C_{27}H_{24}$: 348.1878. Found: 348.1875.

2-(4-Hexyl-phenylethynyl)anthracene (HPEA). ^{1}H NMR (300 MHz, CDCl3): δ 8.41 (s, 2H), 8.24 (s, 1H), 8.05−7.97 (m, 3H), 7.57−7.49 (m, 5H), 7.3 (d, 2H, J = 8.1 Hz), 2.68 (t, 2H, J = 7.65 Hz), 1.65−1.58 (m, 2H), 1.34−1.39 (m, 6H), 0.94 (t, 3H, J = 6.75 Hz). HRMS: calcd for $C_{28}H_{26}$: 362.2034. Found: 362.2031.

2-(4-Heptyl-phenylethynyl)anthracene (HPPEA). The reaction applied to the synthesis of EPEA was conducted using 1-bromo-4-propyl-benzene. Yield: 1.44 g (49%). ^{1}H NMR (300 MHz, $CDCl_3$): δ 8.41 (s, 2H), 8.23 (s, 1H), 8.04−7.97 (m, 3H), 7.56−7.48 (m, 5H), 7.23−7.20 (d, 2H), 2.68−2.63 (t, 2H), 1.67−1.62 (m, 2H), 1.35−0.31 (t, 8H), 0.93−0.89 (t, 3H). HRMS: calcd for $C_{29}H_{28}$: 376.2191. Found: 376.2187.

2-(4-Decyl-phenylethynyl) anthracene (DPEA). The reaction applied to the synthesis of EPEA was conducted using 1-bromo-4-propyl-benzene. Yield: 1.46 g (52%). ^{1}H NMR (300 MHz, $CDCl_3$): δ 8.41 (s, 2H), 8.23 (s, 1H), 8.04−7.97 (m, 3H), 7.56−7.47 (m, 5H), 7.22−7.20 (d, 2H), 2.67−2.62 (t, 2H), 1.67−1.62 (m, 2H), 1.51−1.28 (d, 14H), 0.92−0.88 (t, 3H). HRMS: calcd for $C_{32}H_{34}$: 418.2661. Found: 418.2663.

Fabrication and Characterization of the OFET Devices. Top-contact OFETs were fabricated on a common gate prepared using highly *n*-doped silicon with a 100 nm thick thermally grown SiO_2 dielectric layer. The hydrophobic octyltrichlorosilane monolayer was treated in toluene solution for 2 h. Solutions of the organic semiconductors were spin-coated at 2000 rpm from 0.7 wt % chloroform solutions to form thin films with a nominal thickness of 40−50 nm, as confirmed using a surface profiler (Alpha Step 500, Tencor). Gold source and drain electrodes were evaporated on top of the semiconductor layers (100 nm). All measurements were conducted using channel lengths (L) of 160 μm and channel widths (W) of 1600 μm. The electrical characteristics of the FETs were measured in air using Keithley 2400 and 236 source/measure units. Field-effect mobilities were extracted in the saturation regime from the slope of the source−drain current. 1D XRD studies were performed at the Pohang Accelerator Laboratory (beamline 5A), and synchrotron-based 2D GIWAXS experiments were performed at the Pohang Accelerator Laboratory (beamline 9A).

■ ASSOCIATED CONTENT

Ⓢ Supporting Information

TGA and DSC of the anthracene derivatives. This material is available free of charge via the Internet at http://pubs.acs.org.

■ AUTHOR INFORMATION

Corresponding Authors

*S.-K. Kwon. E-mail: skwon@gnu.ac.kr.
*C. E. Park. E-mail: cep@postech.ac.kr.
*Y.-H. Kim. E-mail: ykim@gnu.ac.kr.

Author Contributions

⊥Jang Yeol Back and Tae Kyu An contributed equally to this work as first authors.

Notes

The authors declare no competing financial interest.

■ ACKNOWLEDGMENTS

This work was supported by a grant (2011-0031639 and 2012M3A6A5055225) from the Center for Advanced Soft Electronics under the Global Frontier Research Program of the Ministry of Education, Science and Technology, Korea. This work was also supported by a grant from the National Research Foundation of Korea (NRF), funded by the Korean Government (MSIP) (2014R1A2A1A05004993 and 2012M3A7B4049647).

■ REFERENCES

(1) Zhang, F.; Hu, Y.; Schuettfort, T.; Di, C.-a.; Gao, X.; McNeill, C. R.; Thomsen, L.; Mannsfeld, S. C. B.; Yuan, W.; Sirringhaus, H.; Zhu, D. Critical Role of Alkyl Chain Branching of Organic Semiconductors in Enabling Solution-Processed N-Channel Organic Thin-Film Transistors with Mobility of up to 3.50 cm^2 V^{-1} s^{-1}. *J. Am. Chem. Soc.* **2013**, *135*, 2338−2349.

(2) Kang, I.; An, T. K.; Hong, J.-a.; Yun, H.-J.; Kim, R.; Chung, D. S.; Park, C. E.; Kim, Y.-H.; Kwon, S.-K. Effect Of Selenophene in a DPP Copolymer Incorporating a Vinyl Group for High-Performance Organic Field-Effect Transistors. *Adv. Mater.* **2013**, *25*, 524−528.

(3) Uoyama, H.; Goushi, K.; Shizu, K.; Nomura, H.; Adachi, C. Highly Efficient Organic Light-Emitting Diodes from Delayed Fluorescence. *Nature* **2012**, *492*, 234−238.

(4) So, K. H.; Kim, R.; Park, H.; Kang, I.; Thangaraju, K.; Park, Y. S.; Kim, J. J.; Kwon, S.-K.; Kim, Y.-H. Synthesis and Characterization of a New Iridium(III) Complex with Bulky Trimethylsilylxylene and Applications for Efficient Yellow-Green Emitting Phosphorescent Organic Light Emitting Diodes. *Dyes Pigm.* **2012**, *92*, 603−609.

(5) Cha, H.; Lee, G. Y.; Fu, Y.; Kim, Y. J.; Park, C. E.; Park, T. Simultaneously Grasping and Self-Organizing Photoactive Polymers for Highly Reproducible Organic Solar Cells with Improved Efficiency. *Adv. Energy Mater.* **2013**, *3*, 1018−1024.

(6) Kim, H. G.; Jo, S. B.; Shim, C.; Lee, J.; Shin, J.; Cho, E. C.; Ihn, S.-G.; Choi, Y. S.; Kim, Y.; Cho, K. Synthesis and Photovoltaic Properties of Benzo[1,2-b:4,5-b′]dithiophene derivative-based Polymers with Deep HOMO Levels. *J. Mater. Chem.* **2012**, *22*, 17709−17717.

(7) Chung, D. S.; Kong, H. Effect of Solvent on Detectivity of Solution-Processed Polymer Photodetectors. *Opt. Lett.* **2013**, *38*, 2814−2817.

(8) Yiming, W.; Xiujuan, Z.; Huanhuan, P.; Xiwei, Z.; Yuping, Z.; Xiaozhen, Z.; Jiansheng, J. Large-Area Aligned Growth of Single-Crystalline Organic Nanowire Arrays for High-Performance Photodetectors. *Nanotechnology* **2013**, *24*, 355201.

(9) Afzali, A.; Dimitrakopoulos, C. D.; Breen, T. L. High-Performance, Solution-Processed Organic Thin Film Transistors from a Novel Pentacene Precursor. *J. Am. Chem. Soc.* **2002**, *124*, 8812−8813.

(10) Ito, K.; Suzuki, T.; Sakamoto, Y.; Kubota, D.; Inoue, Y.; Sato, F.; Tokito, S. Oligo(2,6-anthrylene)s: Acene−Oligomer Approach for Organic Field-Effect Transistors. *Angew. Chem., Int. Ed.* **2003**, *42*, 1159−1162.

DOI: 10.1021/am5063103
ACS Appl. Mater. Interfaces 2015, 7, 351−358

(11) Dong, H.; Wang, C.; Hu, W. High Performance Organic Semiconductors for Field-Effect Transistors. *Chem. Commun.* **2010**, *46*, 5211−5222.
(12) Marrocchi, A.; Seri, M.; Kim, C.; Facchetti, A.; Taticchi, A.; Marks, T. J. Low-Dimensional Arylacetylenes for Solution-Processable Organic Field-Effect Transistors. *Chem. Mater.* **2009**, *21*, 2592−2594.
(13) Dost, R.; Ray, S. K.; Das, A.; Grell, M. Oscillator Circuit Based on a Single Organic Transistor. *Appl. Phys. Lett.* **2008**, *93*, 113505−3.
(14) Wu, W.; Liu, Y.; Zhu, D. π-Conjugated Molecules with Fused Rings for Organic Field-Effect Transistors: Design, Synthesis and Applications. *Chem. Soc. Rev.* **2010**, *39*, 1489−1502.
(15) Anthony, J. E. Functionalized Acenes and Heteroacenes for Organic Electronics. *Chem. Rev.* **2006**, *106*, 5028−5048.
(16) Kim, J.; Kim, S. H.; An, T. K.; Park, S.; Park, C. E. Highly Stable Fluorine-Rich Polymer Treated Dielectric Surface for the Preparation of Solution-Processed Organic Field-Effect Transistors. *J. Mater. Chem. C* **2013**, *1*, 1272−1278.
(17) Lee, B.; Wan, A.; Mastrogiovanni, D.; Anthony, J. E.; Garfunkel, E.; Podzorov, V. Origin of the Bias Stress Instability in Single-Crystal Organic Field-Effect Transistors. *Phys. Rev. B* **2010**, *82*, 085302.
(18) Fan, C.-L.; Lin, Y.-Z.; Chiu, P.-C.; Wang, S.-J.; Lee, W.-D. Teflon/SiO_2 Bilayer Passivation for Improving the Electrical Reliability of Pentacene-based Organic Thin-Film Transistors. *Org. Electron.* **2013**, *14*, 2228−2232.
(19) Park, S.; Nam, S.; Kim, L.; Park, M.; Kim, J.; An, T. K.; Yun, W. M.; Jang, J.; Hwang, J.; Park, C. E. Synthesis and Characterization of a Fluorinated Oligosiloxane-Containing Encapsulation Material for Organic Field-Effect Transistors, Prepared via a Non-Hydrolytic Sol−Gel Process. *Org. Electron.* **2012**, *13*, 2786−2792.
(20) Park, J. H.; Lim, H.; Cheong, H.; Min Lee, K.; Chul Sohn, H.; Lee, G.; Im, S. Anisotropic Mobility of Small Molecule-Polymer Blend Channel in Organic Transistor: Characterization of Channel Materials and Orientation. *Org. Electron.* **2012**, *13*, 1250−1254.
(21) Kim, S.-o.; An, T. K.; Chen, J.; Kang, I.; Kang, S. H.; Chung, D. S.; Park, C. E.; Kim, Y.-H.; Kwon, S.-K. H-Aggregation Strategy in the Design of Molecular Semiconductors for Highly Reliable Organic Thin Film Transistors. *Adv. Funct. Mater.* **2011**, *21*, 1616−1623.
(22) Swartz, C. R.; Parkin, S. R.; Bullock, J. E.; Anthony, J. E.; Mayer, A. C.; Malliaras, G. G. Synthesis and Characterization of Electron-Deficient Pentacenes. *Org. Lett.* **2005**, *7*, 3163−3166.
(23) Melucci, M.; Favaretto, L.; Zambianchi, M.; Durso, M.; Gazzano, M.; Zanelli, A.; Monari, M.; Lobello, M. G.; De Angelis, F.; Biondo, V.; Generali, G.; Troisi, S.; Koopman, W.; Toffanin, S.; Capelli, R.; Muccini, M. Molecular Tailoring of New Thieno(bis)-imide-based Semiconductors for Single Layer Ambipolar Light Emitting Transistors. *Chem. Mater.* **2013**, *25*, 668−676.
(24) Tang, Q.; Li, H.; He, M.; Hu, W.; Liu, C.; Chen, K.; Wang, C.; Liu, Y.; Zhu, D. Low Threshold Voltage Transistors Based on Individual Single-Crystalline Submicrometer-Sized Ribbons of Copper Phthalocyanine. *Adv. Mater.* **2006**, *18*, 65−68.
(25) Barlow, S.; Odom, S. A.; Lancaster, K.; Getmanenko, Y. A.; Mason, R.; Coropceanu, V.; Brédas, J.-L.; Marder, S. R. Electronic and Optical Properties of 4H-Cyclopenta[2,1-b:3,4-b′]bithiophene Derivatives and Their 4-Heteroatom-Substituted Analogues: A Joint Theoretical and Experimental Comparison. *J. Phys. Chem. B* **2010**, *114*, 14397−14407.
(26) Tang, W.; Singh, S. P.; Ong, K. H.; Chen, Z.-K. Synthesis of Thieno[3,2-b]thiophene Derived Conjugated Oligomers for Field-Effect Transistors Applications. *J. Mater. Chem.* **2010**, *20*, 1497−1505.
(27) Usta, H.; Kim, C.; Wang, Z.; Lu, S.; Huang, H.; Facchetti, A.; Marks, T. J. Anthracenedicarboximide-based Semiconductors for Air-Stable, N-Channel Organic Thin-Film Transistors: Materials Design, Synthesis, and Structural Characterization. *J. Mater. Chem.* **2012**, *22*, 4459−4472.
(28) An, T. K.; Kang, I.; Yun, H.-j.; Cha, H.; Hwang, J.; Park, S.; Kim, J.; Kim, Y. J.; Chung, D. S.; Kwon, S.-K.; Kim, Y.-H.; Park, C. E. Solvent Additive to Achieve Highly Ordered Nanostructural Semi-crystalline DPP Copolymers: Toward a High Charge Carrier Mobility. *Adv. Mater.* **2013**, *25*, 7003−7009.
(29) Ye, Q.; Chi, C. Recent Highlights and Perspectives on Acene based Molecules and Materials. *Chem. Mater.* **2014**, *26*, 4046−4056.
(30) An, T. K.; Park, S.-M.; Nam, S.; Hwang, J.; Yoo, S.-J.; Lee, M.-J.; Yun, W. M.; Jang, J.; Cha, H.; Hwang, J.; Park, S.; Kim, J.; Chung, D. S.; Kim, Y.-H.; Kwon, S.-K.; Park, C. E. Thin Film Morphology Control via a Mixed Solvent System for High-Performance Organic Thin Film Transistors. *Sci. Adv. Mater.* **2013**, *5*, 1323−1327.
(31) Desiraju, G. R.; Gavezzotti, A. From Molecular to Crystal Structure; Polynuclear Aromatic Hydrocarbons. *J. Chem. Soc., Chem. Commun.* **1989**, 621−623.
(32) Jang, S. H.; Kim, H.; Hwang, M. J.; Jeong, E. B.; Yun, H. J.; Lee, D. H.; Kim, Y. H.; Park, C. E.; Yoon, Y. J.; Kwon, S. K.; Lee, S. G. Solution Processable Symmetric 4-Alkylethynylbenzene End-Capped Anthracene Derivatives. *Bull. Korean Chem. Soc.* **2012**, *33*, 541−548.
(33) Aleshin, A. N.; Lee, J. Y.; Chu, S. W.; Kim, J. S.; Park, Y. W. Mobility Studies of Field-Effect Transistor Structures Based on Anthracene Single Crystals. *Appl. Phys. Lett.* **2004**, *84*, 5383−5385.
(34) Murphy, A. R.; Fréchet, J. M. J. Organic Semiconducting Oligomers for Use in Thin Film Transistors. *Chem. Rev.* **2007**, *107*, 1066−1096.
(35) Zhang, F.; Melzer, C.; Gassmann, A.; Seggern, H. v.; Schwalm, T.; Gawrisch, C.; Rehahn, M. High-Performance N-Channel Thin-Film Transistors with Acene-based Semiconductors. *Org. Electron.* **2013**, *14*, 888−896.
(36) Yun, H.-J.; Chung, D. S.; Kang, I.; Park, J. W.; Kim, Y.-H.; Kwon, S.-K. Novel Triethylsilylethynyl Anthracene-based Organic Semiconductors for High Performance Field Effect Transistors. *J. Mater. Chem.* **2012**, *22*, 24924−24929.
(37) Mei, J.; Diao, Y.; Appleton, A. L.; Fang, L.; Bao, Z. Integrated Materials Design of Organic Semiconductors for Field-Effect Transistors. *J. Am. Chem. Soc.* **2013**, *135*, 6724−6746.
(38) Ito, K.; Suzuki, T.; Sakamoto, Y.; Kubota, D.; Inoue, Y.; Sato, F.; Tokito, S. Oligo(2,6-anthrylene)s: Acene−Oligomer Approach for Organic Field-Effect Transistors. *Angew. Chem.* **2003**, *115*, 1191−1194.
(39) Brocks, G.; van den Brink, J.; Morpurgo, A. F. Electronic Correlations in Oligo-Acene and -Thiopene Organic Molecular Crystals. *Phys. Rev. Lett.* **2004**, *93*, 146405.
(40) Payne, M. M.; Parkin, S. R.; Anthony, J. E.; Kuo, C.-C.; Jackson, T. N. Organic Field-Effect Transistors from Solution-Deposited Functionalized Acenes with Mobilities as High as 1 $cm^2/V{\cdot}s$. *J. Am. Chem. Soc.* **2005**, *127*, 4986−4987.
(41) Zhao, Q.; Kim, T. H.; Park, J. W.; Kim, S. O.; Jung, S. O.; Kim, J. W.; Ahn, T.; Kim, Y.-H.; Yi, M. H.; Kwon, S.-K. High-Performance Semiconductors based on Alkoxylnaphthyl End-Capped Oligomers for Organic Thin-Film Transistors. *Adv. Mater.* **2008**, *20*, 4868−4872.
(42) Kim, H.-S.; Kim, Y.-H.; Kim, T.-H.; Noh, Y.-Y.; Pyo, S.; Yi, M. H.; Kim, D.-Y.; Kwon, S.-K. Synthesis and Studies on 2-Hexylthieno-[3,2-b]thiophene End-Capped Oligomers for OTFTs. *Chem. Mater.* **2007**, *19*, 3561−3567.
(43) Halik, M.; Klauk, H.; Zschieschang, U.; Schmid, G.; Ponomarenko, S.; Kirchmeyer, S.; Weber, W. Relationship between Molecular Structure and Electrical Performance of Oligothiophene Organic Thin Film Transistors. *Adv. Mater.* **2003**, *15*, 917−922.
(44) Kitamura, C.; Abe, Y.; Kawatsuki, N.; Yoneda, A.; Asada, K.; Kobayashi, T.; Naito, H. Influence of Alkyl Chain Length on the Solid-State Packing and Fluorescence of 1,4,5,8-Tetra(alkyl)anthracenes. *Mol. Cryst. Liq. Cryst.* **2007**, *474*, 119−135.
(45) Chen, J.; Subramanian, S.; Parkin, S. R.; Siegler, M.; Gallup, K.; Haughn, C.; Martin, D. C.; Anthony, J. E. The Influence of Side Chains on the Structures and Properties of Functionalized Pentacenes. *J. Mater. Chem.* **2008**, *18*, 1961−1969.
(46) Nguyen, T.-Q.; Martini, I. B.; Liu, J.; Schwartz, B. J. Controlling Interchain Interactions in Conjugated Polymers: The Effects of Chain Morphology on Exciton−Exciton Annihilation and Aggregation in MEH−PPV Films. *J. Phys. Chem. B* **2000**, *104*, 237−255.
(47) An, T. K.; Jang, S. H.; Kim, S.-O.; Jang, J.; Hwang, J.; Cha, H.; Noh, Y. R.; Yoon, S. B.; Yoon, Y. J.; Kim, L. H.; Chung, D. S.; Kwon, S.-K.; Kim, Y.-H.; Lee, S.-G.; Park, C. E. Synthesis and Transistor Properties of Asymmetric Oligothiophenes: Relationship between

DOI: 10.1021/am5063103
ACS Appl. Mater. Interfaces 2015, 7, 351−358

Molecular Structure and Device Performance. *Chem.—Eur. J.* **2013**, *19*, 14052−14060.
(48) Chen, S.; Sun, B.; Hong, W.; Aziz, H.; Meng, Y.; Li, Y. Influence of Side Chain Length and Bifurcation Point on the Crystalline Structure and Charge Transport of Diketopyrrolopyrrole-Quaterthiophene Copolymers (PDQTs). *J. Mater. Chem. C* **2014**, *2*, 2183−2190.
(49) Lei, T.; Wang, J.-Y.; Pei, J. Roles of Flexible Chains in Organic Semiconducting Materials. *Chem. Mater.* **2013**, *26*, 594−603.
(50) Mei, J.; Bao, Z. Side Chain Engineering in Solution-Processable Conjugated Polymers. *Chem. Mater.* **2014**, *26*, 604−615.
(51) Zhang, J.; Tan, L.; Jiang, W.; Hu, W.; Wang, Z. N-Alkyl Substituted Di(perylene bisimides) as Air-Stable Electron Transport Materials for Solution-Processible Thin-Film Transistors with Enhanced Performance. *J. Mater. Chem. C* **2013**, *1*, 3200−3206.
(52) Kang, I.; Yun, H.-J.; Chung, D. S.; Kwon, S.-K.; Kim, Y.-H. Record High Hole Mobility in Polymer Semiconductors via Side-Chain Engineering. *J. Am. Chem. Soc.* **2013**, *135*, 14896−14899.
(53) Pei, J.; Wang, X.-Y.; Zhuang, F.-D.; Zhou, X.; Yang, D.-C.; Wang, J.-Y. Influence of Alkyl Chain Length on the Solid-State Properties and Transistor Performance of BN-Substituted Tetrathienonaphthalenes. *J. Mater. Chem. C* **2014**, *2*, 8152−8161.
(54) An, T. K.; Hahn, S. H.; Nam, S.; Cha, H.; Rho, Y.; Chung, D. S.; Ree, M.; Kang, M. S.; Kwon, S. K.; Kim, Y. H.; Park, C. E. Molecular Aggregation-Performance Relationship in the Design of Novel Cyclohexylethynyl End-Capped Quaterthiophenes for Solution-Processed Organic Transistors. *Dyes Pigm.* **2013**, *96*, 756−762.
(55) Kim, C.; Huang, P.-Y.; Jhuang, J.-W.; Chen, M.-C.; Ho, J.-C.; Hu, T.-S.; Yan, J.-Y.; Chen, L.-H.; Lee, G.-H.; Facchetti, A.; Marks, T. J. Novel Soluble Pentacene and Anthradithiophene Derivatives for Organic Thin-Film Transistors. *Org. Electron.* **2010**, *11*, 1363−1375.
(56) Spano, F. C. Excitons in Conjugated Oligomer Aggregates, Films, and Crystals. *Annu. Rev. Phys. Chem.* **2006**, *57*, 217−243.
(57) Park, J.-H.; Lee, D. H.; Kong, H.; Park, M.-J.; Jung, I. H.; Park, C. E.; Shim, H.-K. Organic Thin-Film Transistor Properties and the Structural Relationships between Various Aromatic End-Capped Triisopropylsilylethynyl Anthracene Derivatives. *Org. Electron.* **2010**, *11*, 820−830.
(58) Hunter, C. A.; Sanders, J. K. M. The Nature of π-π Interactions. *J. Am. Chem. Soc.* **1990**, *112*, 5525−5534.
(59) Tsuzuki, S.; Honda, K.; Uchimaru, T.; Mikami, M.; Tanabe, K. Origin of Attraction and Directionality of the π/π Interaction: Model Chemistry Calculations of Benzene Dimer Interaction. *J. Am. Chem. Soc.* **2001**, *124*, 104−112.
(60) Jeong, Y. J.; Jang, J.; Nam, S.; Kim, K.; Kim, L. H.; Park, S.; An, T. K.; Park, C. E. High-Performance Organic Complementary Inverters Using Monolayer Graphene Electrodes. *ACS Appl. Mater. Interfaces* **2014**, *6*, 6816−6824.
(61) Choi, D.; Ahn, B.; Kim, S. H.; Hong, K.; Ree, M.; Park, C. E. High-Performance Triisopropylsilylethynyl Pentacene Transistors via Spin Coating with a Crystallization-Assisting Layer. *ACS Appl. Mater. Interfaces* **2012**, *4*, 117−122.
(62) Amin, A. Y.; Khassanov, A.; Reuter, K.; Meyer-Friedrichsen, T.; Halik, M. Low-Voltage Organic Field Effect Transistors with a 2-Tridecyl[1]benzothieno[3,2-b][1]benzothiophene Semiconductor Layer. *J. Am. Chem. Soc.* **2012**, *134*, 16548−16550.

DOI: 10.1021/am5063103
ACS Appl. Mater. Interfaces 2015, 7, 351−358